Wide Area Real Time Kinematics with Galileo and GPS Signals

Manuel Hernández-Pajares, J.Miguel Juan, Jaume Sanz, Raül Orús, *Res. Gr. Astron. Geomatics, gAGE/UPC, Barcelona, Spain*
Alberto García-Rodríguez, *ESTEC/ESA, Nordwijk, The Netherlands*
Oscar L.Colombo, *GEST/NASA GSFC Code 926, Greenbelt, Maryland, USA*

BIOGRAPHIES

Dr. Manuel Hernández-Pajares is an associate professor of the Department of Applied Mathematics IV at the Technical University of Catalonia (UPC) from 1993. He started working on GPS in 1989 for the cartographic and surveying applications. His focus has been in the area of GNSS ionospheric determination and precise radionavigation, since 1995. He is the Ionosphere WG chairman and Ionospheric product coordinator of the International GPS Service (IGS) since 2002.

Dr. J. Miguel Juan Zornoza is an associate professor of the Department of Applied Physics at the Technical University of Catalonia (UPC). His current research interest is in the area of GPS ionospheric tomography, GPS data processing algorithms, and radionavigation.

Dr. Jaume Sanz Subirana is an associate professor of the Department of Applied Mathematics IV at the Technical University of Catalonia (UPC). His current research interest is in the area of GPS ionospheric tomography, GPS data processing algorithms, and radionavigation.

Mr. Raül Orús is Ph.D student on Aerospace Science at gAGE/UPC. His work is focused on the developement of algorithms to compute and validate Global Ionospheric Maps (GIMs) from GNSS data.

Mr. Alberto Garcia has a degree in Telecommunications Engineering from the T.U. of Madrid. He has been involved in satellite navigation activities since 1996, working at GMV for several projects related with the EGNOS system design and validation. Since 2000, he has been working at ESA in the areas of receiver design and navigation algorithms.

Dr. Oscar L. Colombo works in the area of applications of space geodesy, including gravity field mapping, spacecraft orbit determination, and precise positioning by space techniques, mostly for the Space Geodesy Branch (Code 926) of NASA Goddard Space Flight Center. In recent years, he has developed and tested techniques for very long baseline kinematic GPS, in collaboration with groups in Australia, Denmark, Holland, and the USA.

ABSTRACT

The main factor limiting the range extension of the Real Time Kinematics technique beyond few tens of kilometers is the differential ionospheric correction between the roving and the nearest reference GNSS station. Such ionospheric correction impedes the real-time ambiguity fixing, and the corresponding accurate navigation at the sub-decimeter level.

In this paper, the authors present the recent developments in the application of accurate real-time ionospheric corrections in the context of the future three-frequency systems, such as Galileo and Modernized GPS, regarding previous studies (Hernandez-Pajares et al. 2003b). Indeed, from new datasets gathered in the new three-frequency signal simulator placed at ESTEC/ESA, the feasibility of the Wide Area Real Time Kinematics is confirmed, mostly in single epoch mode (instantaneously): the navigation can be typically performed with few centimeters of error at distances of hundreds of kilometers from the nearest Galileo or Modernized GPS reference station. The new improved strategy adopted (WARTK-3.2) includes a no-differenced approach, the ionospheric corrections integrity monitoring, and the capability of the roving user orientation determination with one single antenna at the level of few degrees of error. Moreover, the results obtained with the corresponding strategy adapted to the dual-frequency GPS data confirm both the previous results and the new capabilities of the technique. Particularly, several datasets have been analyzed. Firstly real GPS data have been studied corresponding to an experiment of urban navigation (UNBAR01), performed at Barcelona, Spain, in 2001, with Solar Maximum conditions and local ionospheric perturbations. On the other hand, several three-frequency datasets, simulated in radio-frequency, have been analyzed as well with WARTK-3.2, including a car and an aircraft, moving around the NE of Spain, at distances around 200 km away from the nearest reference site. The results show the

feasibility of the long-range real-time accurate positioning with errors of few centimeters, mostly in single-epoch in the new satellite navigation systems.

INTRODUCTION

The capability of providing a real-time GNSS positioning service with errors below ten centimeters at regional and continental scale strongly depend on the capability to accurately estimate the differential ionospheric corrections between GNSS receivers separated by hundreds of kilometers: The differential ionospheric refraction limits the real-time subdecimeter navigation at distances lower than 10-20 km from the nearest reference site (RTK technique, implemented in many brands of dual-frequency GPS receivers), impeding the carrier phase ambiguity fixing to the right integer value.

Experiment	Shortest baseline/km Rover/Fixed	Ionospheric Activity	Fixed Rec. Ambiguity success %	Roving Rec. Ambiguity success (%	Kind of rover	Region	Dates	Reported in
BellKin99	116 / 286	Mid.Solar Cycle & Quite	97	80-100	4x4 Car	Catalonia, NE Spain	23-03-99	Colombo et al. 99 (ION)
NWPacific1	400/900	Mid Solar Cycle & Active high lat. (Kp=6)	90-100	80	IGS Site	NWCanada-USA	03-05-98	Hernández et al. 00a, Colombo et al. 00 (GRL, PLANS)
NWPacific2	162/900	Mid-Low Solar Cycle & Irreg.	95-100	80-90	IGS Site	NWCanada-USA	28-04 to 01-05-98	Hernández et al. 00b (ION)
SolarMax1	130/500	Solar Maximum	85-95	80	IGS Site	Central Europe	19 to 22-04-00	Hernández et al. 01a (GRL)
SolarMax2	130/500	Solar Max. & Supestorm	50-95	80	IGS Site	Central Europe	12 to 15-07-00	Hernández et al. 00b (ION)
Baltic99	144/285	Travelling Iono. Disturb. (TIDs)	97	83	IGS Site	North Europe	25-08-99	Hernández et al. 01b (ION)
Equator01	1000-3000/.	Solar Max. & Equator & Very Active (Kp to 9)	90	---	IGS Sites	Central Asia to Oceania	06-03 to 02-04-01	Hernández et al. 02a (JGR)
TCARdata (simulated)	130/300	Solar Max.	100	92 (single-epoch)	Sim. car	Central Europe	17-03-00 (noon)	Hernández 03a-b (IEEE-TGARS, Navigation)
UNBAR01	70-115/100	Solar Max. & Strong TIDs	100	~80 (with integrity)	Car	Barcelona, NE Spain	11-06-01	This paper
WARTK3 Lab.Test 1-2	178-238 /250-600	Solar Max.	100	100 (single-epoch)	1:Car 2:Air.	Iberian Peninsula	31-03-90 (ionos.)	This paper
WARTK3 Lab. Test 3	404/250-600	Solar Max.	100	99 (single-epoch)	Fixed Site	Iberian Peninsula	31-03-90 (ionos.)	This paper

Table 1: **Summary of experiments performed to test the Wide Area Real-Time Kinematics concept.**

Indeed, the Ionosphere produces ambiguity estimation biases and correlations whose mitigation is the main problem of several techniques such as LAMBDA method (Teunissen et al. 1997) which takes into account these correlations in order to get reliable ambiguities for short baselines. With this present state-of-the-art technique, we would need about 500 reference receivers to provide service to a country such as Spain. And several thousands would be needed to provide service to Europe. And this is unaffordable from the logistic and economic points of view. To solve this limitation, the authors started to explore, several years ago, a direct approach by providing to the users a very accurate ionospheric refraction estimate to be removed from the user navigation filter equations. This was fulfilled by developing a very precise technique to compute ionospheric corrections in real-time using a 3-D voxel model of the ionosphere, estimated by means of a Kalman filter, and using exclusively GNSS data gathered from fixed receivers separated several hundreds of kilometers (see Hernández-Pajares et al. 1999b, 2000a and summary of performed experiments in Table 1). In this way, just few dozens of fixed reference GNSS receivers are enough to ensure a sub-decimeter positioning service at continental scale, over Europe for example. One potential network to support this service could be that which is deployed to support EGNOS, the European meter-level positioning system fulfilling integrity requirements to be used in civil aviation (see for instance Ventura-Traveset et al. 2001).

The main feature of this new technique was patented for GPS dual-frequency data in 1999 (Wide Area RTK, WARTK, UPC-Patent Nbr.9902585). And the extension to three-frequency systems such as Galileo, and Modernized GPS were developed in the context of a previous project funded by ESA in 2002 (WARTK for 3 frequencies, or WARTK-3, ESA Patent Nbr.02-12627). In such new technique, the ionospheric filter was combined with the TCAR algorithm (Harris 1997), allowing most part of the time an instantaneous correct fixing of ambiguities with receivers separated more than one hundred km. This was one of the main advantages of WARTK-3 in respect to WARTK-2 (or WARTK for two-frequencies systems), the potential achievement of instantaneous (at single-epoch) subdecimeter positioning at long distance (see details in Hernández-Pajares et al. 2002b, 2003b).

In this work, the main goal has been the consolidation and improvement of WARTK-3 algorithm, using both actual GPS data and additional realistic three-frequency data sets, generated ad-hoc by the authors with the new Galileo signal frequency generator. Such data has served to analyze the performance of the proposed algorithm, which introduces two main improvements: (1) A new approach to maintain the integrity of the ionospheric corrections broadcasted to the users also in the presence of ionospheric perturbations, and (2) the integration of the 3 carriers ambiguity fixing in a WARTK-3 zero-differenced (undifferenced) user navigation filter. In this way, we can take advantage of: (a) the redundance from a simultaneous real-time positioning and ambiguity estimation, and (b) the availability of new estimates to the users, among the positions, such as the orientation change ("wind-up") with a single antenna. This improved approach incorporates new capabilities regarding the previous techniques as it is depicted in Table 2.

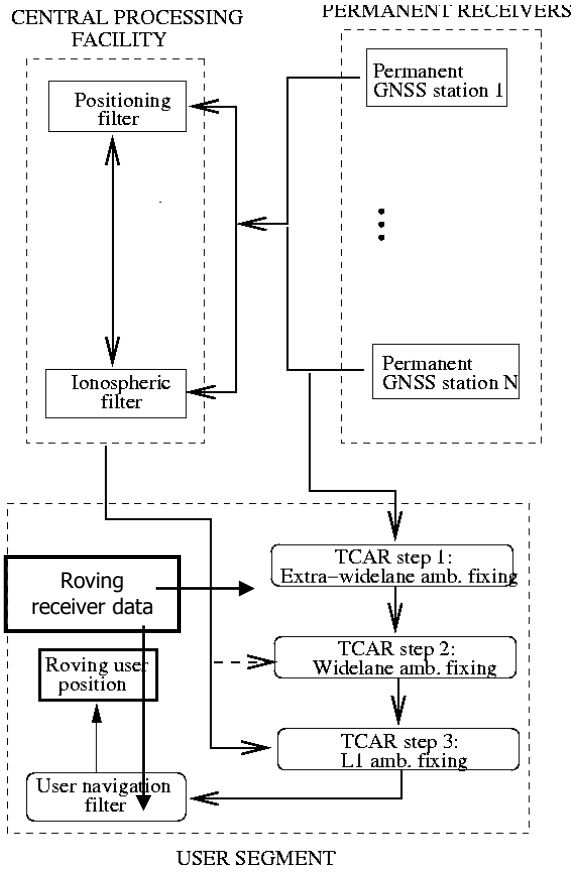

Figure 1: Layout of the original WARTK-3 algorithm, which incorporates the accurate real-time ionospheric corrections to the TCAR approach of solving the ambiguities from the longest to the shortest wavelength in a geometry-free way (see details of the WARTK-3 approach at Hernández-Pajares et al. 2003b).

FIRST IMPROVEMENT: INTEGRITY OF THE IONOSPHERIC CORRECTIONS

One of the most difficult scenarios that sometimes appears at mid-latitudes is the presence of ionospheric waves (Traveling Ionospheric Disturbances, TIDs) in the GNSS Wide Area network. They produce a non-linear behavior of the Ionosphere, which can affect the interpolation performance of the differential ionospheric delays between the reference stations (see for example

Orús et al. 2003). This interpolation capability is usually essential to provide accurate values to the roving users in the Wide Area network. One way to overcome -or at least mitigate- these problems is the use of a real-time ionospheric filter by the roving user (Hernández-Pajares et al. 2001b, 2002b). Moreover we have improved the WARTK-3 and WARTK techniques, by incorporating a gradient step detector of the ionospheric differential delay in the reference stations. Such improvement is going to be briefly described in the next section. The performance of this approach has been studied using real GPS data gathered in Spain (see below). The results suggest a significant improvement in the problem when the gradient step detector is used.

Gradient method description

Once the unambiguous Slant Total Electron Content (STEC) is computed in the reference stations, these values can be used to provide, through an interpolation, the STEC value for any user in the coverage area. The method of interpolation will depend on the size of the area as well as the ionospheric conditions. For instance, in small networks (i.e. distances up to few hundreds of kilometers) and quiet ionospheric conditions, the interpolated STEC value for the user can be obtained by combining the corresponding values in the reference stations with fixed weights.

Method	**ADVANTAGES**	**DISADVANTAGES**
TCAR	Low computational load.	Seriously limited by ionospheric refraction. Certain effect of pseudorange multipath.
ITCAR	Improved results by integrating TCAR in a navigation filter.	The ionospheric delay still limits the 3er ambiguity fixing.
FMCAR	Improved design and results by using "federated" Kalman Filters and as many carriers as available.	The ionospheric delay still limits the technique to short baselines.
WARTK (2-freq.)	Accurate real-time ionospheric modelling, allows precise navigation at hundreds of kilometers from the nearest reference site .	In spite of speeding-up the navigation Kalman filter, a significant convergence time is still needed (5-15 minutes).
WARTK-3	Uses the extra-widelane, and an accurate real-time iono. model to provide single-epoch precise navigation capabilities, and greatly speeding up the convergence of the Navigation Filter to just few epochs.	Certain effect of pseudorange multipath.
WARTK-3.2	Use of an integrated user zero-differenced navigation filter being more iono-perturbation tolerant and code multipath immune, and providing orientation change estimation to single antenna users.	

Table 2: Main advantages and disadvantages of the four real-time ambiguity resolution procedures discussed in this work: TCAR (Harris 1997), Integrated TCAR (Vollath et al. 2001), FMCAR (Vollath 2004), WARTK and WARTK-3 (Hernández-Pajares et al. 2000a and 2003b), and WARTK-3.2 (this work).

In this work, and for each satellite in view from the reference stations, a planar (or quadratic) adjustment is made by estimating the 2 (or 5) components of the between-station single STEC difference gradient. From this gradient (or gradient and Hessian), any user in the coverage area can compute its own single difference of STEC with respect to the reference stations for a given satellite. This is done in this way because the pierce points of the satellites in view from a regional network appear clustered differently for each satellite reproducing the geometry of the network but in different ionospheric regions, and with different gradients in general (see Figure 2). This is useful to interpolate easily to the position of the roving receivers.

The main advantage of this approach is that we can include in the gradient computation additional information as ionospheric models and temporal continuity. And this allows the system to monitor the quality of this planar adjustment in the reference stations in order to detect ionospheric irregularities such as TIDs, avoiding its direct effect on the users.

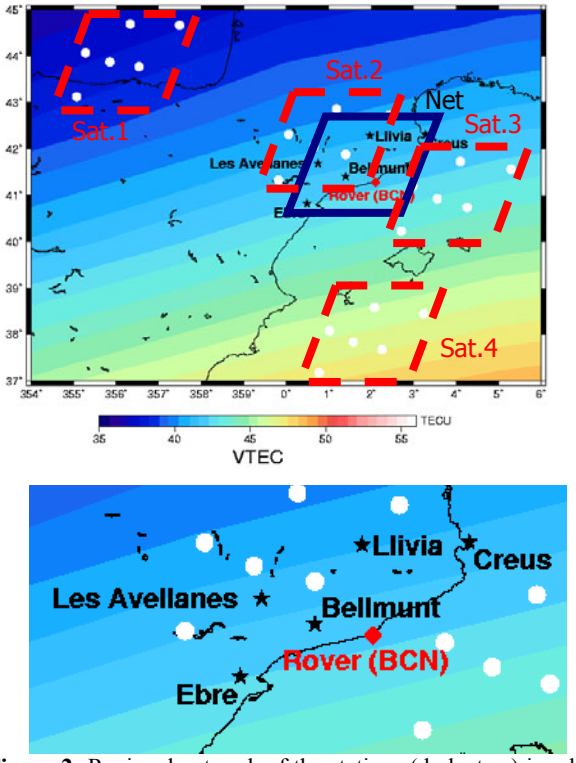

Figure 2: Regional network of the stations (dark stars) involved in the GPS experiment UNBAR01 (general view, topside, zoom, bottomside). Such stations have been used to test the new algorithms proposed in this paper. The roving stations were

placed in Barcelona, NE Spain (red diamond). The pierce points of 2 high elevation satellites in view, merged in corresponding clusters, are also indicated with white circles, as far as the TEC distribution over the region (at 13 UT approximately of day 162, 2003).

SECOND IMPROVEMENT: INTEGRATION OF WARTK-3 IN A NAVIGATION FILTER (WARTK-3.2)

The user algorithm, which integrates WARTK-3 in a unique navigation filter, is represented in Figure 3 and it can be briefly described for the different components indicated in such layout:

Step 1 "Roving Receiver Data": The algorithm is fed with data measured with a Galileo or Modernized GPS receiver. These data consist of 3 carrier phase measurements (L1, L2, L3) and 3 code measurements (P1, P2, P3) for each satellite in view, which are used simultaneously during each observation epoch (typically each second). As in the case of the reference stations algorithm, six combinations of these types of observations are used. These are the difference of wide lane and extra-wide lane carrier phases (L_w-L_{ew}), the ionosphere-free carrier-phase combination (L_c), the ionospheric (geometry-free) combination (L_I), the extra-wide lane carrier-phase minus pseudorange difference (L_{ew}-P_{ew}), the wide-lane carrier phase minus pseudorange difference (L_w-P_w) and the ionosphere-free pseudorange combination P_c. If the user does not choose to calculate his/her own ionospheric model (this is usually not necessary), the geometric-free observations L_I are only used to compute the ambiguity ionospheric carrier phase combination B_I from the STEC computed and provided externally.

Step 2 "Network Data and corrections": Beside the data from its own receiver, the user must receive data and differential corrections from the network of reference stations. These data are: (1) The same six combinations of measurements as in the rover but only from one reference station receiver. These measurements are necessary in order to compute satellite clocks and to fix integer values of double differenced ambiguities. And (2), the single-differenced STEC for each satellite in view is interpolated to the rover position from the surrounded reference stations STECs. These values are broadcast jointly with a parameter of quality indicating the confidence of the ionospheric correction.

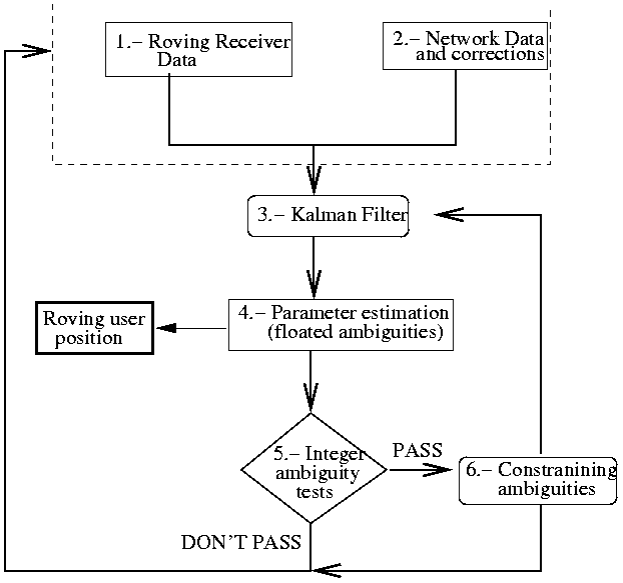

Figure 3: WARTK-3.2 algorithm layout for the roving user.

Step 3 "Kalman Filter": The observable equations are approximated by a linear expansion in a rover position computed from a standard positioning technique using pseudorange data. They are solved in the framework of a forward Kalman Filter.

The data from the receiver and from the network are modelled taking into account the following main features:

1) The program runs on absolute mode (without double differencing the measurements, i.e. zero-differenced). The initial disadvantage of this approach is that it implies a more complex model and it is necessary to estimate more parameters such as the wind-up, delay code biases and satellite and receiver clocks that mostly cancel out when double differences are made. The advantages, on the one hand, are that we can, and we do, estimate the parameters (such as the wind-up, providing the rover orientation change) and on the other hand, that we can use any additional information of these parameters that would improve the estimations of the overall unknowns, in particular the real-time position.

2) Note that the estimation of the antenna orientation is only possible from the equation on the ionospheric carrier phase combination LI: although the wind-up appears on the Lc equation, it cannot be distinguished from the rover clock parameter. The reason is that the effect is essentially the same for all the satellites when the rover is moving horizontally.

3) With this procedure, the satellite clocks are referred to the reference station clock. In order to maintain these values as close as possible to the GPS time, it is necessary to send the estimation of the reference station clock to the user.

Steps 4 "Parameter estimation" and 5 "Integer ambiguity tests": Once the filter provides estimations for the ambiguities, the following step is to fix double-differenced ambiguities to its integer values. Several tests are made in order to maximize the probability of fixing these ambiguities to their correct values. Such tests mainly look at the widelane ambiguity formal and round-up error, quality of transmitted differential ionospheric correction and ambiguity parity checks for GPS data. In general, the checking and fixing of ambiguities with three-frequencies are performed going from the longest to the shortest wavelength, fixing and updating the covariance each time the tests are passed.

Step 6 "Constraining ambiguities": From the integer values of L1, Lw and Lew double differenced ambiguities, the corresponding ionospheric and ionosphere-free ambiguities can be estimated and introduced as additional constraints in the Kalman filter in order to improve the parameter estimation of the next epoch.

RESULTS WITH ACTUAL GPS DATA: UNBAR01 EXPERIMENT

In order to test the performance of the improved technique, two main datasets have been used. They consist on actual GPS measurements and signal-simulated observables in 3-frequencies. The first dataset corresponds to the GPS Urban Navigation in Barcelona, Spain – 2001 experiment (hereinafter UNBAR01) which was performed the 11th of June, 2001, coinciding with Solar Maximum conditions. Two roving receivers placed on the roof of a car at a distance of about 77.5 cm were gathering data on a trail of several km in Barcelona city. And a set of permanent receivers belonging to the Cartographical Institute of Catalonia (CATNet) was used in the computation of the differential corrections in real-time mode with the WARTK technique (see Figure 2). The difficulty of this scenario is still higher due to the presence of ionospheric waves (TIDs) and to the outer position of the roving station regarding the reference network. Thus the two potential improvements in WARTK-3 described above have been tested:

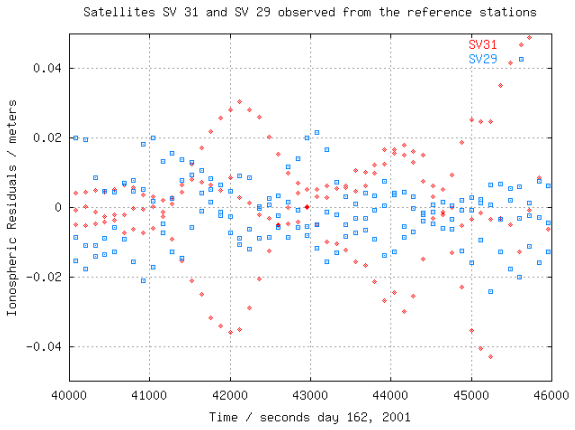

Figure 4: Ionospheric residual (true-planar fit model) computed at the reference stations for satellites SV/PRN31 (red crosses) and SV/PRN29 (blue squares).

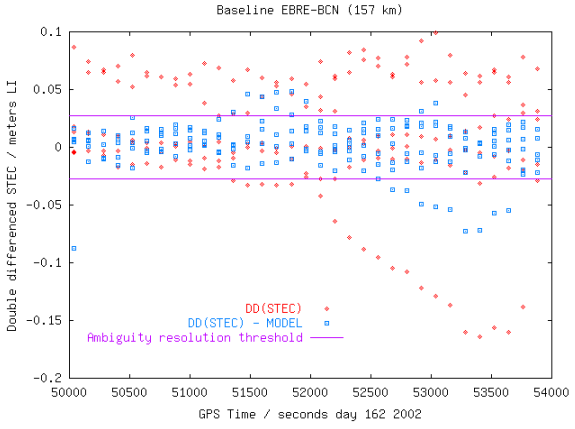

Figure 5: Double differenced STEC values (red) of the roving receiver, and the corresponding residuals after applying the reference net broadcast values (blue), for more than one hour in the UNBAR01 experiment.

An improved filtering approach of bad ionospheric corrections

The main results are summarized in several representative figures below. At Figure 2 you can see the layout of the reference and rover stations used in this study and the typical TEC variation during the experiment. As an example, the ionospheric residual regarding the planar fit for SV/PRN31 (affected by the ionospheric waves, see Figure 4) is anomalously high compared with the remaining ones, in such a way that it can be detected, flagged and eventually eliminated from the broadcast message to the users, using the above described gradient method. And the positioning accuracy attains values below 10 cm after few epochs at more than 100 km from the nearest reference site. This is achieved in a difficult scenario with Traveling Ionospheric Disturbances after using the corresponding ionospheric corrections (WARTK technique for GPS data).

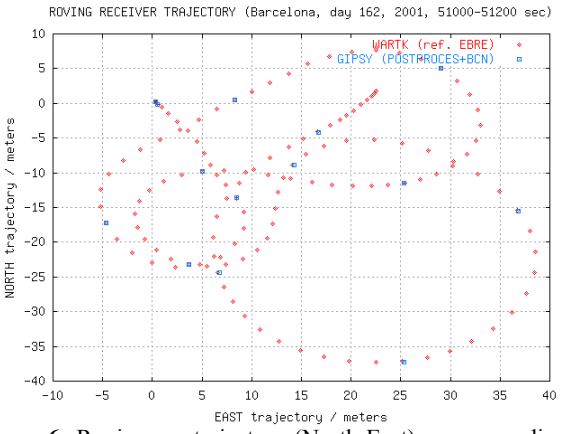

Figure 6: Roving car trajectory (North-East), corresponding to the same experiment, but with the car in movement, for two minutes. The red trajectory has been computed with WARTK being the closest station, Bellmunt, at 67 km away. And the reference trajectory (blue) is computed with GIPSY software (in post-process and using very close reference station data).

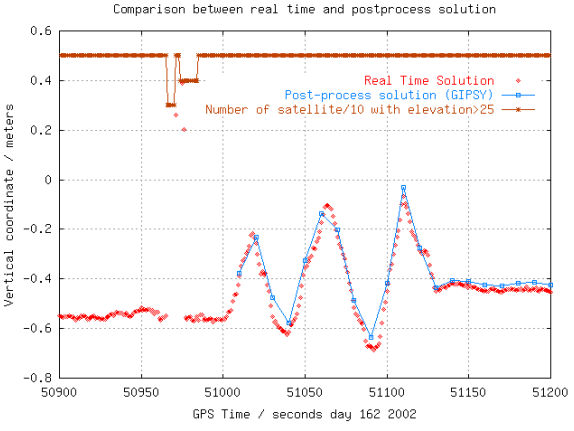

Figure 7: Plot showing the vertical component (Up), for five-minutes of the car movement in the UNBAR01 experiment. It corresponds, approximately, to the horizontal movement estimated in

Figure 6.

User zero-differenced navigation filter

The double differenced ionospheric values of the rover are represented as a function of the time (Figure 5), as far as the error after substracting the interpolated ionospheric corrections from the network of stations. The necessity of using broadcast accurate ionospheric corrections can be seen. The main results are summarized from

Figure **6** to Figure 8. The trajectory of the car is compared with the post-process solution using the JPL software GIPSY (see for instance Webb and Zumberge, 1997), using additional data coming from a very close reference station (BCN) at few kilometers away. This post-processed solution is obtained every 10 seconds. A good agreement of about few centimeters of WARTK can be seen using Bellmunt as the closest reference station, at about 70 km away. In

Figure **6** and Figure 7: we show the horizontal and vertical results during a typical period of movement (for 120 consecutive seconds), with an agreement at the level of several centimeters.

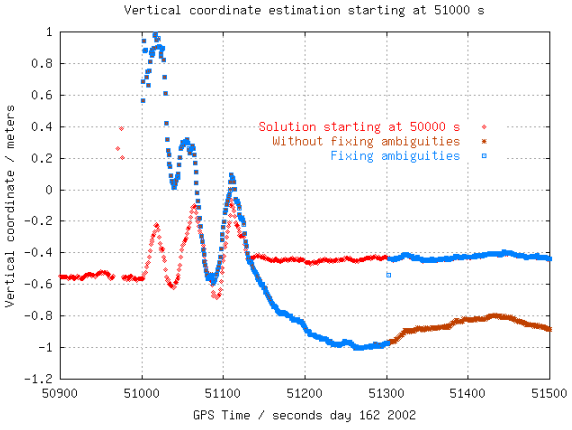

Figure 8: Plot similar to the last plot, showing the vertical component (Up), but after a general lost of satellites, fixing ambiguities at 51300s (blue) and floating ambiguities (brown).

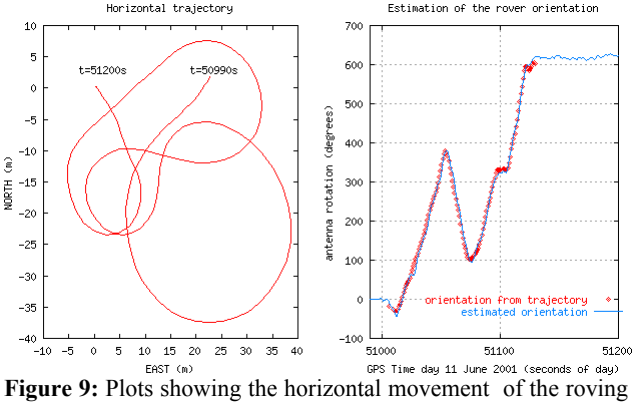

Figure 9: Plots showing the horizontal movement of the roving receiver, during a part of the UNBAR01 experiment (left side plot). At the right hand plot, the corresponding wind-up estimation (blue) compared with the value derived from the trajectory (red) are shown.

In Figure 7 and Figure 8, we can see the real-time vertical component of the trajectory (red) computed by WARTK compared with a corresponding reference post-processed solution (blue): Figure 7 illustrate the case of 3 simultaneous cycle-slips, in such a way that the positioning around the epoch 50970s must be done with only 1 fixed double difference and 4 available satellites. Some few very bad estimates have been filtered out in real-time mode as well, by means of the positioning sigma computed by the user. After these epochs, the positioning error quickly returns to just few centimeters. On the other hand, Figure 8 corresponds to a "cold start" in epoch 51000s, and approximately 150s later, 3 ambiguities are fixed and the positioning achieves the centimeter error level. However, the solution without fixing ambiguities

(Figure 8 as well) shows an error of several decimeters, slowly converging to the right positions. Finally, in Figure 9 the horizontal movement and corresponding wind-up estimated from the ionospheric measurements are represented. These results are compatible at the measurement error level of few degrees.

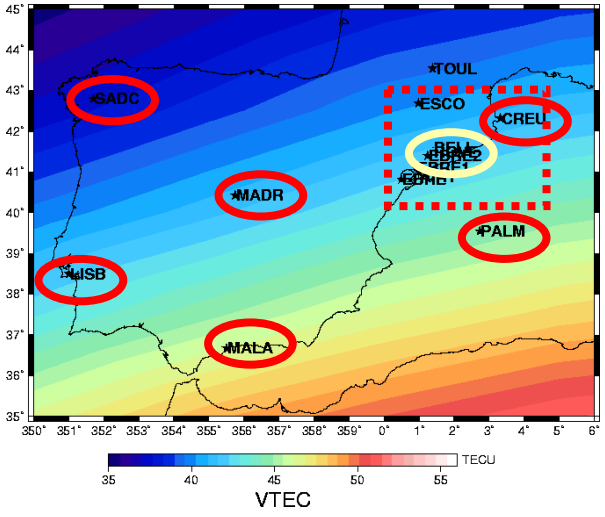

Figure 10: Scenario (a) layout –yellow ellipse=rover, red ellipse=fixed-.

RESULTS WITH 3-FREQUENCIES

Several datasets were simulated in the RNEU GSVF facility (Figure 12, see document P6908-35-011), during the days from 26 to 30 January 2004 at ESTEC/ESA, in the context of the present "WARTK-3 Laboratory Test Campaign" project. These datasets were used to characterize the performance of the WARTK-3.2 technique describe before.

The GNSS receiver used the data gathered at frequencies corresponding to E1 (1.589742 GHz, wavelength of 18.9 cm, also called S1) and E2 (1.256244 GHz, wavelength of 23.9cm, also called S2), in conjunction with S3 (1.561098 GHz, wavelength of 19.2 cm), to be able to compute an extra-wide lane combination (see below).

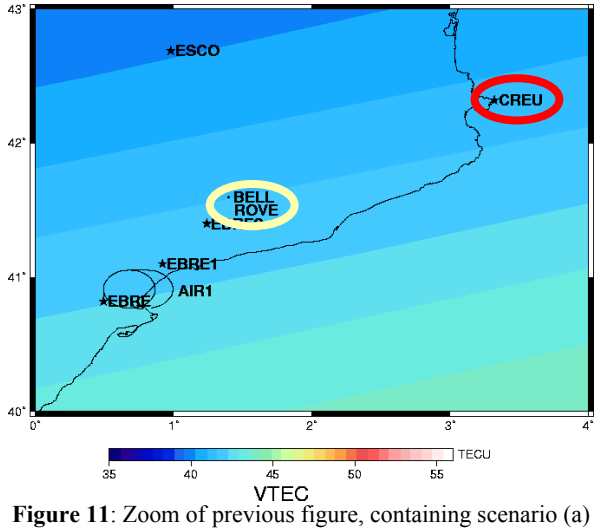

Figure 11: Zoom of previous figure, containing scenario (a) layout –yellow ellipse=rover, red ellipse=fixed-.

Figure 12: Galileo Signal Simulation Facility, ESTEC/ESA, Nordwijk, The Netherlands (GSVF, courtesy of Thales).

From the carrier phases S1, S2 and S3, and pseudoranges, P1, P2 and P3, everything in meters, the following combinations are used:

(1) Ionospheric combination, S_i = S1 - S2 P_i = P2 - P1

(2) Ionospheric-free combination of S1 and S2,

$$S_c = \frac{f_1^2 S_1 - f_2^2 S_2}{f_1^2 - f_2^2} \quad P_c = \frac{f_1^2 P_1 - f_2^2 P_2}{f_1^2 - f_2^2}$$

(3) The wide-lane combination S_w (wavelength λ_w= 0.90 m),

$$S_w = \frac{f_1 S_1 - f_2 S_2}{f_1 - f_2} \quad P_w = \frac{f_1 P_1 + f_2 P_2}{f_1 + f_2}$$

(4) The extra wide-lane combination (λ_e =10.47m),

$$S_e = \frac{f_1 S_1 - f_3 S_3}{f_1 - f_3} \quad P_e = \frac{f_1 P_1 + f_3 P_3}{f_1 + f_3}$$

The summary of the results obtained applying the improved WARTK3.2 technique has been divided into three main sub-sections corresponding to the three analyzed scenarios: (a) surface rover (ROVE) navigating

at 178 km from the nearest reference station (NRS), (b) air rover (AIR1) navigating at 238 km from the NRS, and (c) fixed receiver (MADR) navigated as real rover, at 404 km away from the NRS. The WARTK-3 resulting performance of the real-time ionospheric corrections provided to the user and the corresponding real-time positioning will be detailed in the worst case scenario under Solar-Maximum Ionosphere conditions. The error in GPS orbit is not simulated because its value can be typically removed at the cm-level or better, by adjusting the orbits with the permanent network data and/or using predicted accurate orbits.

Scenario (a): Surface rover (ROVE) results

One surface rover receiver (ROVE) was simulated, navigating in Catalonia at the NE part of Spain. The closest reference receiver used was CREU, at 178 km away (see Figure 10 and Figure 11, being the additional fixed stations used TOUL, PALM, MADR, SADC, LISB and MALA), and the worst case ionospheric scenario under Solar Maximum conditions was considered.

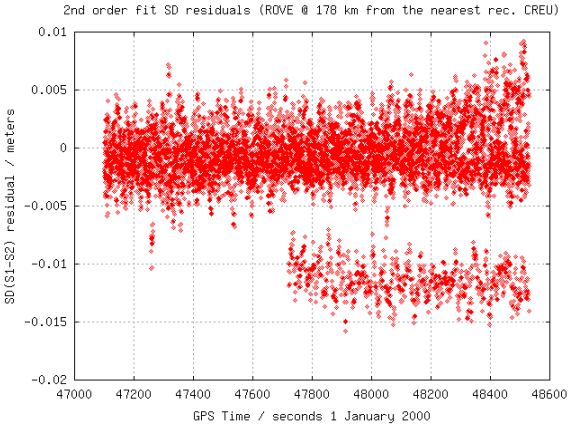

Figure 13: Double-differenced ionospheric refraction user errors when a second-order (quadratic) fit is used in the interpolation (scenario (a)).

The first point which performance has been analyzed is the error of the real-time ionospheric corrections provided to the user (or interpolation problem). The International Reference Ionosphere model (IRI, Bilitza 1990) has been used to simulate the ionospheric delays. Such model predicts realistic ionospheric refraction values, but without considering ionospheric waves (Traveling Ionospheric Disturbances, TIDs), which were covered in the integrity study performed above. Moreover, we have concentrated our study on the ionospheric interpolation problem, by considering that the carrier phase ambiguities between the reference permanent GNSS stations can be fixed correctly in real-time (this has been proven with actual GPS up to baselines of thousands of kilometers, see Hernández-Pajares et al. 2002a).

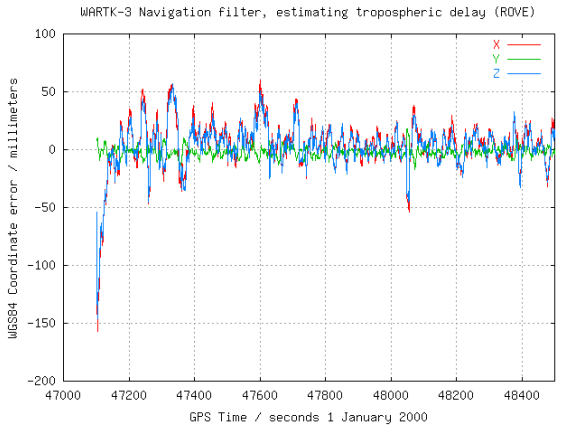

Figure 14: ROVE WARTK3 Navigation: X,Y,Z errors (scen. a).

One important result obtained in this scenario is that with the corresponding high ionospheric values, a planar fit (commented above in "Gradient method description") is not accurate enough for the interpolation task. However a 2nd order (quadratic) interpolation procedure of the between-stations single differences is accurate enough to guarantee the achievement of errors below the exigent limit of 2.5 cm of the ionospheric combination, S1-S2=S_i. This is due to the high values and variations achieved by the ionospheric refraction in the Solar Maximum scenario and, the sometimes strong ionospheric slant TEC variation of the rays coming from the South and crossing tails of the Equatorial Anomalies. Indeed, in this scenario, the user ionospheric interpolation error decreases when we pass from using planar fit (below 7cm) to using quadratic interpolation (below 2cm, Figure 13). In this way, with the quadratic interpolation, 100% of real-time interpolated double-differenced STEC at ROVE are below the threshold value of 2.5cm[1] of Si (RMS of 0.5 cm).

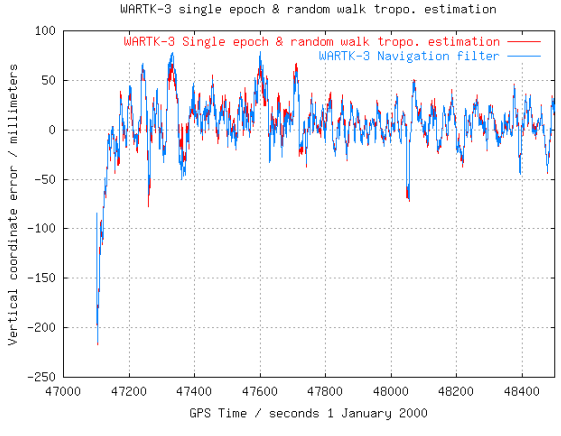

Figure 15: ROVE WARTK3.2 single-epoch Navigation treating the vertical tropospheric wet delay such as a random walk (X,Y,Z errors, scenario (a)).

[1] $(\lambda_2-\lambda_1)/2$, see Hernández-Pajares et al. 2000a.

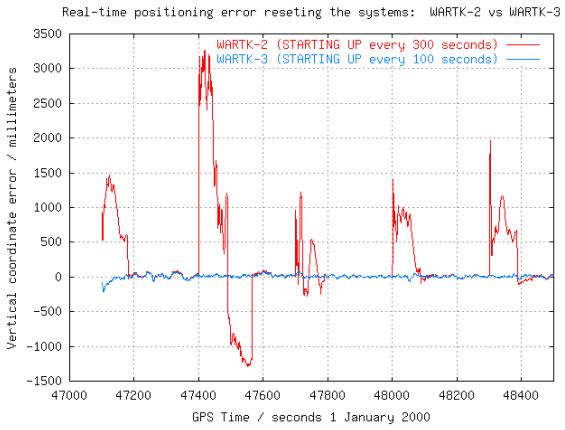

Figure 16: WARTK3.2 vs WARTK-2 WGS84 Vertical (up) positioning error for ROVE in scenario (a), starting up everything each 100/300 sec. respectively (including tropo.).

As was proposed in the first part of this study, the user will apply the ionospheric corrections received from the fixed stations network in the framework of a general navigation Kalman filter feed with zero-differenced (undifferenced) observations. With 3-frequencies measurements 100% of ambiguities are fixed since the beginning and the real-time positioning error decrease below 10 cm after a convergence time of just few seconds, needed to decorrelate the tropospheric delay[2] (Figure 14).

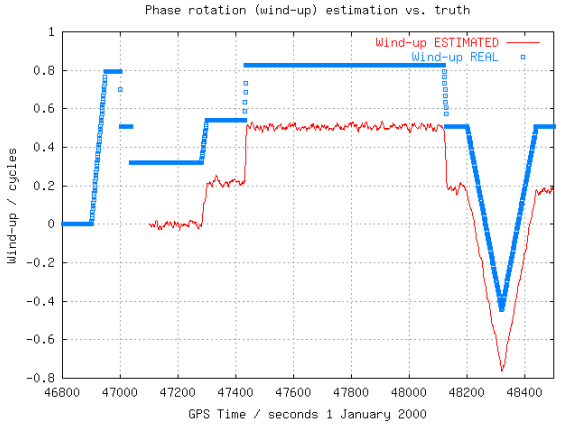

Figure 17: Real-time phase orientation change estimation (wind-up) in ROVE (red) vs. the real one (blue).

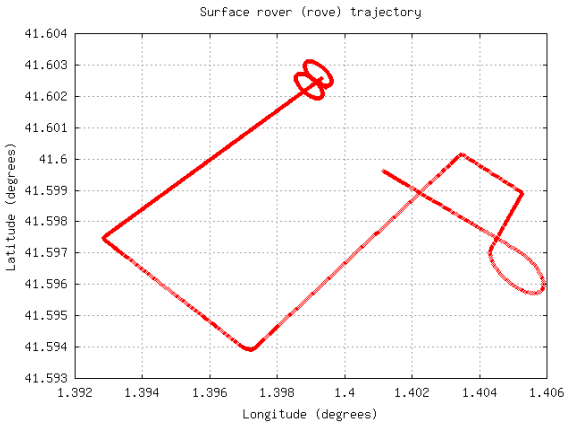

Figure 18: Horizontal projection of the ROVE trajectory, which is reflected in the wind-up values to be estimated.

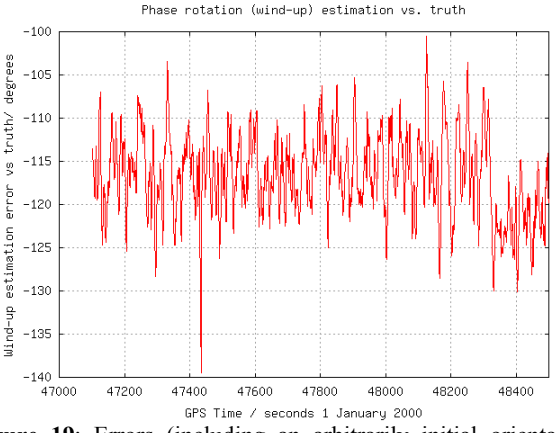

Figure 19: Errors (including an arbitrarily initial orientation value) of the antenna rotation instantaneous estimation for car ROVE in scenario (a).

The results are practically equivalent in single epoch mode (with an RMS of 1.4 cm) emulated as a continuous cold start (setting up all the variances to ∞), but maintaining the random walk tropospheric estimation (see for instance the vertical component error in Figure 15). We have studied as well the corresponding performance with 2-frequencies systems in order to compare with 3-frequencies systems. Indeed, when we simulate a cold starting-up with two-frequencies data, we get as well a sub-decimeter real-time positioning such as with three-frequencies (RMS of 2 cm and 100% amb. fixed), but after a convergence time of approximately 100 sec (time needed for both ambiguity fixing and initial tropospheric state estimation), instead of instantaneously (Figure 16). This result is in concordance with that obtained with actual GPS data. The corresponding positioning errors for ROVE moving around the scenario (a) are lower than 6 cm, obtaining a RMS of 2,4 cm (3-D), with an RMS of 1.7, 0.4 and 1.5 cm in X,Y,Z components, respectively.

As it was commented above WARTK-3.2 provides, simultaneously to the rover position, an estimate of the antenna orientation change (wind-up) by comparing its

[2] The navigation has been started at 47100 sec, coinciding with the simulator availability of common satellites.

own ambiguous undifferenced STEC with the external ionospheric correction gathered from the network. It can be seen in Figure 17 and Figure 19 that the single rover antenna orientation change (wind-up) is estimated in real-time with an RMS of 4.8 degrees being the corresponding maneuvers plotted in Figure 18 (the offset is meaningful because it corresponds to an arbitrarily initial reference orientation).

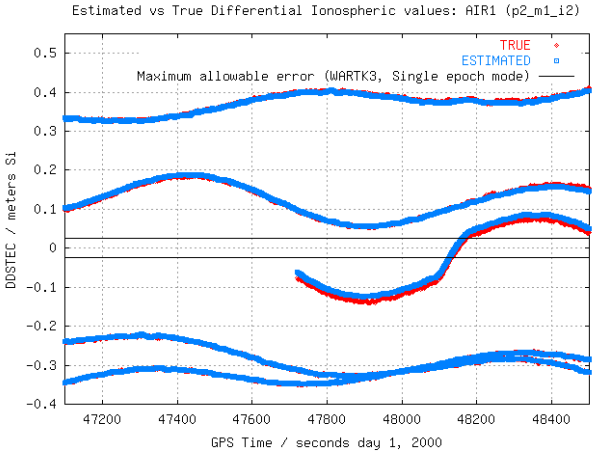

Figure 20: Estimated (blue) vs. actual differential ionospheric values corresponding to the satellites in view from the rover AIR1 (scenario (b)).

Scenario (b): Airplane roving receiver (AIR1) results

In order to show the performance of WARTK-3.2 used with GNSS receivers under high dynamics, we have analyzed the scenario (b) corresponding to an airplane describing several turns in the same region (Catalonia at NE Spain) as the surface rover, close to EBRE, which has not used in the computations (see Figure 11 and Figure 21). In this case, the nearest reference receiver (PALM) is located at about 238 km away from the airplane which flies again in the worst case of the ionospheric scenario under Solar Maximum conditions.

For the airplane AIR1, we can see in Figure 20 the effect of the high dynamics of the receiver which produces important non-linear variations of the differential ionospheric values. In spite of this wave-like variation, the 100% of real-time interpolated differential STECs at AIR1 is below the threshold value of 2.5 cm (RMS of 0.5 cm, see Figure 20 as well).

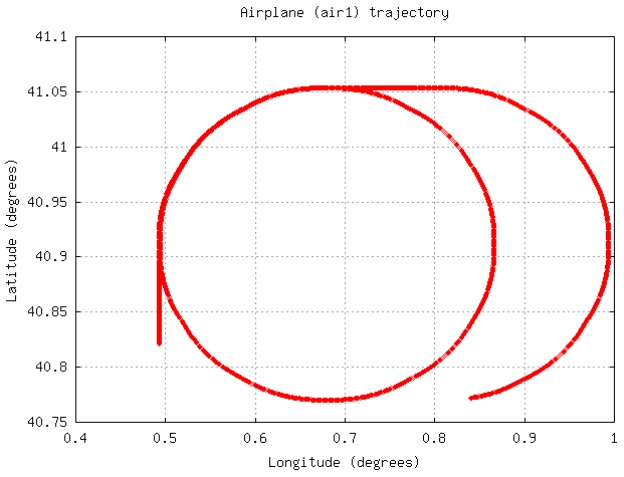

Figure 21: Horizontal projection of the AIR1 trajectory.

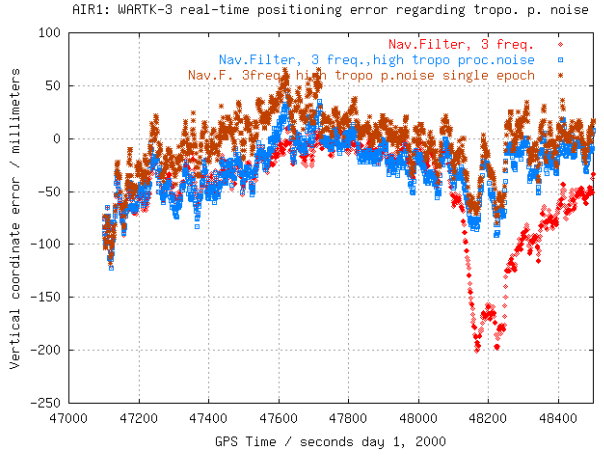

Figure 22: WARTK-3.2 Vertical coordinate error compared between using a standard ground-based tropospheric random-walk process noise (red), and using a higher process noise (blue and brown in single-epoch mode as well).

One of the points in the accurate real-time positioning of airplanes is the high rate of height change producing high variations of tropospheric delay, converting its accurate estimation in an issue that can affect seriously the navigation quality. This point is clear in Figure 22, where WARTK-3.2 with the standard permanent receiver random process noise for the vertical tropospheric delay produces a significant error in periods with strong height changes of the airplane (such as 48100-48200 sec, see Figure 23 as well). The accuracy improves significantly (sub-decimeter values) when more freedom (higher random process noise) is applied to the troposphere, both in navigation filter and single-epoch modes (see again Figure 22).

Scenario (c): Long distance results (MADR)

A third scenario has been studied in order to characterize the performance of WARTK-3.2, in particular the

accurate interpolation of ionospheric corrections, at still longer distances and maintaining the Solar Maximum ionospheric conditions. In this scenario MADR, fixed station treated as rover is located at 404 km away from EBRE, the nearest fixed site (see Figure 10). In spite of the long distance and Solar-Maximum scenario, 98.7% of real-time interpolated double-differenced STEC at MADR is below the threshold value of 2.5cm of Si (RMS value of 0.8 cm, Figure 24).

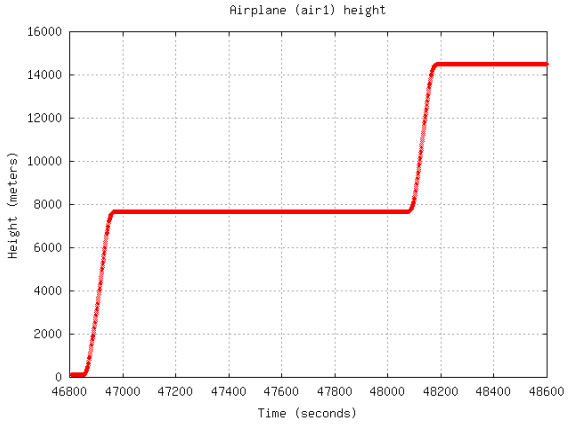

Figure 23: Height evolution corresponding to the GNSS receiver (AIR1) on-board an aircraft, in scenario (b).

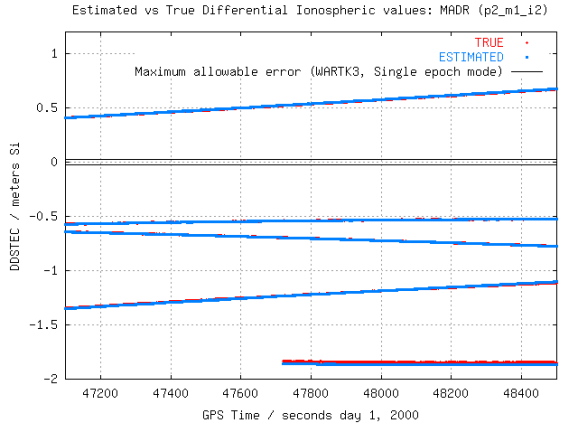

Figure 24: Estimated (blue) vs. actual differential ionospheric values corresponding to the satellites in view from the fixed station MADR treated as rover at more than 400 km from the nearest reference site (scenario (b)).

The navigation error is still maintained at few-centimeters error level. After ~30 sec. (mostly required for estimating the tropospheric delay), an RMS of 1 cm is achieved for the more difficult vertical coordinate (Figure 25), being the 100% of ambiguities fixed since the beginning.

SUMMARY OF DIFFERENT RESULTS

The main results are summarized in Table 3 for one typical case with medium values of tropospheric and multipath and high values of ionospheric differential refraction. Worst case scenarios for the real-time filter and single-epoch navigation have been also considered, including high tropospheric variation and high multipath with extreme measurement noise. RMSs of 2 and 0.5 cm for vertical and horizontal positioning are attained for both real-time navigation filter and single-epoch mode after an initial period of about 20 seconds to estimate the initial tropospheric state in such nominal case. In the case of the navigation filter the worst results are obtained with high tropospheric variation in the airplane scenario (RMSs of 4 and 3 cm in vertical and horizontal components). The worst results occurs in single epoch mode with high multipath for the receiver ROVE, and for the largest baselines. Both results are related with a miss-functioning of the signal simulator that produce extremely high values of carrier phase noise (in terms of an irrealistic multipath) that affect mainly the resolution of the wide-lane ambiguity, not the shortest carrier phase ambiguity. Note that this problem is not related with the proposed algorithm and would appear also with short baselines and classical techniques such as RTK. Despite this, in these two cases a subdecimeter error-level navigation in more than 90% of the epochs, it is possible to mitigate this problem just by waiting for some epochs before fixing the ambiguities. For example, waiting just 5 seconds practically 100% of the ambiguities can be fixed correctly.

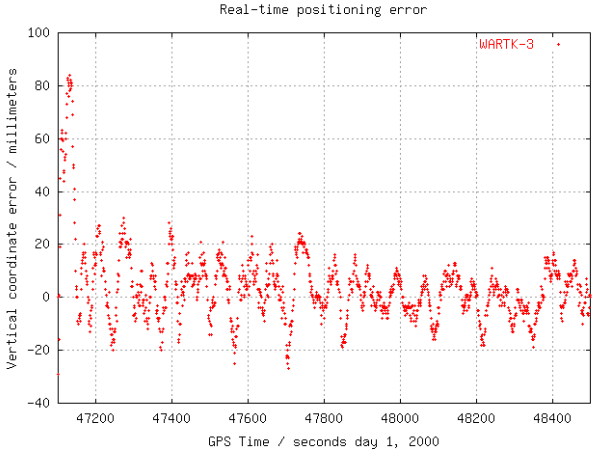

Figure 25: Vertical coordinate error of WARTK-3.2 for the fixed station MADR treated as rover at 404 km away from the nearest reference site (EBRE) and in Solar Maximum ionospheric conditions.

CONCLUSIONS

An improved approach of Wide Area Real Time Kinematics (WARTK) with 2 and 3 GNSS frequencies has been presented, including the design and testing with real GPS data and simulated GALILEO signals. The

inclusions of a gradient step detection approach, and the integration of the WARTK-3 algorithm in a user navigation filter scheme –which include some novel approaches such as the simultaneous user orientation parameters for one single antenna- are two new features among others of WARTK-3.2.

The good performance of WARTK-3.2 has been shown firstly with GPS data (WARTK-2), and in a difficult scenario from both points of views: the ionosphere (Solar Maximum and local perturbations) and the navigation in an urban scenario, at the outer part of the network. The improved technique WARTK-3.2 has been tested as well with 3-frequencies datasets generated by the authors in the new Galileo signal generator, within Solar Maximum conditions at mid latitude, in three scenarios: car, airplane and fixed station treated as rovers, at 178, 238 and 404 km away from the corresponding nearest reference site.

Another new result summarized in this work is the real-time orientation change performed at the level of 5 degrees of RMS (Figure 19) by the roving user with a single antenna thanks to the ionospheric broadcasted corrections and the zero-differenced approach to solve the navigation state.

The results confirm previous studies: WARTK3.2 makes a new navigation service feasible with errors of few centimeters from national and continental networks of GNSS stations separated by hundreds of km. This accurate real-time positioning can be typically achieved instantaneously with 3-frequency systems (such as Galileo and Modernized GPS). With the current GPS the accurate (centimeter error level) can be obtained in real-time, but after the best part of 1-2 minutes during a receiver cold start. The results obtained so far suggest the maturity of the WARTK technique in order to built a first prototype based on the EGNOS (or other SBAS systems) RIMS data stream, gathered through Internet (SiSNET/INSPIRE, Torán-Martí and Ventura-Traveset, 2004).

ACKNOWLEDGMENTS

The authors of this report are grateful to the Cartographical Institute of Catalonia (ICC) and to the International GPS Service (IGS), to make publicly available several GPS datasets used in this work. This work has been performed under ESA/ESTEC Contract Number 15453/01/NL/LvN-CCN01, being Alberto García-Rodríguez the contractor manager.

REFERENCES

Billitza D., International Reference Ionosphere 1990, URSI/COSPAR, NSSDC/WDC-A-R&S 90-22, 1990.

Colombo O., Hernández-Pajares M., Juan J.M., Sanz J., J. Talaya, Resolving carrier-phase ambiguities on-the-fly, at more than 100Km from the nearest reference, with the help of ionospheric tomography, Awarded oral presentation, Institute of Navigation GPS'99, Nashville (USA), 1999.

Colombo O., Hernández-Pajares M., Juan J.M., Sanz J., Ionospheric tomography helps resolve GPS ambiguities On The Fly at distances of hundreds of kilometers during increased geomagnetic activity, PLANS 2000, San Diego, USA, 2000.

Colombo O., Hernández-Pajares M., J.M. Juan, J. Sanz, Wide-Area, carrier-phase ambiguity resolution using a tomographic model of the Ionosphere, Navigation, 49(1) p. 61-69, 2002.

Harris, R.A.: Direct Resolution of Carrier-Phase Ambiguity by 'Bridging the Wavelength Gap', ESA Publication "TST/60107/RAH/Word", 2/1997.

Hernández-Pajares M., J.M. Juan, J. Sanz and O.L. Colombo, Precise ionospheric determination and its application to real-time GPS ambiguity resolution, Institute of Navigation ION GPS'99, Nashville, Tennessee, USA, September 1999b.

Hernández-Pajares, M., J.M. Juan, J. Sanz and O.L. Colombo, Application of ionospheric tomography to real-time GPS carrier-phase ambiguities resolution, at scales of 400-1000 km, and with high geomagnetic activity, Geophysical Research Letters, 27, 2009-2012, 2000a.

Hernández-Pajares M., Juan J.M., Sanz J., O. Colombo, H. Van der Marel, Precise ionospheric determination and its application to real-time GPS ambiguity resolution, Institute of Navigation ION-GPS'2000, Salt-Lake, USA, 2000b.

Hernández-Pajares M., J.M. Juan, J. Sanz, O. Colombo, and H. van der Marel, A new strategy for real-time integrated water vapor determination in WADGPS networks, Geophysical Research Letters, 28 No.17 p. 3267-3270, 2001a.

Hernández-Pajares, M., J.M. Juan, J. Sanz, O.L. Colombo, Tomographic modeling of GNSS ionospheric corrections: Assessment and real-time applications, ION GPS'2001, Salt Lake, USA, September 2001b.

Hernández-Pajares M., J.M. Juan, J. Sanz and O. Colombo, Improving the real-time ionospheric determination from GPS sites at Very Long Distances over the Equator, Journal of Geophysical Research - Space Physics, (A) Vol. 107, pp.1296-1305, 2002a.

Hernández-Pajares, M., J.M. Juan, J.Sanz, Wide Real Time Kinematics with three-carrier phases (WARTK-3), Final Report, ESA/ESTEC Contract Number 15453/01/NL/LvH, Technical Manager: Alberto García-Rodríguez, September 2002b.

Hernández-Pajares, M., J.M. Juan, J.Sanz, O.L.Colombo, Feasibility of Wide-Area Subdecimeter Navigation With GALILEO and Modernized GPS, IEEE Transactions on Geoscience and Remote Sensing, Vol.41, No.9, September 2003a.

Hernández-Pajares M., Juan J.M., Sanz J., O. Colombo, Impact of Real-Time Ionospheric Determination on Improving Precise Navigation with GALILEO and Next-Generation GPS, NAVIGATION: Journal of The Institute of Navigation, Vol.50, No.3, pp.205-218, Fall 2003b.

Orús, R., M. Hernández-Pajares., J.M. Juan, J.Sanz, Ionospheric Effects on Precise Navigation at Regional and Continental Scales over Europe, ISPRS International Workshop "Theory, Technology and Realities of Inertial / GPS Sensor Orientation", Castelldefels, Spain, 22-23 September 2003.

Teunissen, P. J., C. C. De Jonge, J.M. Tiberius, Performance of the Lambda method for fast GPS ambiguity resolution, Navigation 44(3), 1997.

Torán-Martí F. and J. Ventura-Traveset, The ESA SISNeT Project: Current Status and Future Plans, The European Navigation Conference GNSS 2004.

Ventura-Traveset J., P. Michel, L. Gauthier, Architecture, Mission and Signal Processing Aspects of the EGNOS System: the first European Implementation of GNSS, Seventh International Workshop on Digital Signal Processing Techniques for Space Communications, DSP 2001, Sesimbra, Portugal, 1-3 October 2001.

Vollath, U., E. Roy, Ambiguity Resolution using Three Carriers - Performance Analysis using "Real" Data, GNSS Symposium, Seville, May 2001.

Vollath, U., TCAR Test-2 Final Presentation, GNSS Final Presentations Days, ESTEC/ESA, Nordwijk, April 2004

Webb F.H and J.F. Zumberge, An introduction to GIPSY/OASIS-II, JPL D-11088, 1997.

P6908-35-011-Issue3: GNSS-2 Signal Validation, Receiver to NPU Interface Control Document, Thales Navigation, ESA Contract No. RR029281, 6 November 2001.

	Navigation filter	Single epoch mode

# Exp		Success (%)	Vertical RMS (mm)	Horizonal RMS (mm)	Initial Ambiguity/ Positioning Convergence Time	Success (%)	Vertical RMS (mm)	Horizontal RMS (mm)
3 rove (178 km away)	*Nominal case:* Mid Mult., Mid. Tropo, **High Iono.**	100	24	5	0/20	100	24	6
2 rove-GPS*	*Nominal* in two-frequencies	100	24	5	100	77	1506	380
5 air1 (238 km away)	*Navigation filter worst case:* air1, Mid. Mult., **High Tropo.**, **High Iono**.	100	42	28	0	100	27	8
4 rove	*Single-Epoch worst case*: rove, **High Mult.**, Mid Tropo, **High Iono**.	100	29	10	0/20	100 /Sew 97.7 /Sw 98.6 /S1	429 (91%)	157 (90%)

Table 3 **Selected results summarizing some of the main and worst cases (in the ambiguity success column, an unlabelled percentage refers to a common 100% success rate in three frequencies, otherwise the corresponding frequency is indicated; in vertical and horizontal RMS columns corresponding to single epoch mode, the parenthesis contain the percentage of epochs with 3D positioning error lesser than 10cm).**